

Research Article

Adjustable Scaling Parameters for State of Charge Estimation for Lithium-Ion Batteries Using Iterative Multiple UKFs

Hong Jianwang , Ricardo A. Ramirez-Mendoza , and Jorge de J. Lozoya-Santos

School of Engineering and Sciences, Tecnológico de Monterrey, Monterrey, Mexico

Correspondence should be addressed to Hong Jianwang; 9120180002@jxust.edu.cn

Received 18 July 2019; Revised 27 February 2020; Accepted 12 March 2020; Published 10 April 2020

Academic Editor: Rafael Morales

Copyright © 2020 Hong Jianwang et al. This is an open access article distributed under the Creative Commons Attribution License, which permits unrestricted use, distribution, and reproduction in any medium, provided the original work is properly cited.

In this paper, one unscented Kalman filter with adjustable scaling parameters is proposed to estimate the state of charge (SOC) for lithium-ion batteries, as SOC is most important in monitoring the latter battery management system. After the equivalent circuit model is applied to describe the lithium-ion battery charging and discharging properties, a state space equation is constructed to regard SOC as its first state variable. Based on this state space model about SOC, one state estimation problem corresponding to the nonlinear system is established. In implementing the unscented Kalman filter, state estimation is influenced by the scaling parameter. Then, one criterion function is constructed to choose the scaling parameter adaptively by minimizing this criterion function. To extend one single unscented Kalman filter with adjustable scaling parameters to multiple module estimation, one improved unscented Kalman filter is advised based on iterative multiple models. Generally, the main contributions of this paper consist in two folds: one is to introduce a selection strategy for the scaling parameter adaptively, and the other is to combine iterative multiple models and a single unscented Kalman filter with adjustable scaling parameters. Finally, two simulation examples confirm that our unscented Kalman filter with adjustable scaling parameters and its improved iterative form are better than the classical Kalman filter; i.e., our obtained SOC estimation error converges to zero.

1. Introduction

Lithium-ion battery is the leading energy storage technology for many research fields, such as electric vehicle, modern electric grids, transformation, etc. The main features of lithium-ion batteries include energy density, a long time, and a lower self-discharge rate, so many research studies on these main features of lithium-ion batteries are carried out in recent years from their own different points of view. One interesting area of research is battery state estimation, especially named as state of charge (SOC) estimation, as SOC can not only reflect the remaining capacity of lithium-ion batteries but also embody the performance and endurance mileage of electric vehicles. Furthermore, SOC is the most important factor in the battery management system, which is critical for the safety, efficiency, and life expectancy of lithium-ion batteries. Generally, SOC indicates the remaining battery capacity to show how long the battery will last. It helps the battery management system to protect the

battery from overcharging and over-discharging and makes the energy management system to determine an effective dispatching strategy. But SOC cannot be directly measured using physical sensors; it must be estimated using some newly developed methods with the aid of measurable signals, such as the voltage and current of the battery. In this paper, SOC estimation is our concerned problem for lithium-ion batteries. SOC estimation has been widely studied in recent years, and lots of estimation algorithms have been proposed to acquire precise SOC estimation. As the number of references on SOC estimation is vast, here we only list some main references on this topic as follows. An improved extended Kalman filter method is presented to estimate SOC for vanadium redox battery [1], using a gain factor. Some unknown parameters from the state space model are identified by the classical least squares method. The square root cubature Kalman filter algorithm has been developed to estimate SOC of batteries [2], where $2n$ points are calculated to give the same weight, according to cubature transform to

approximate the mean of state variables. To improve the accuracy and reliability of SOC estimation for battery, an improved adaptive cubature Kalman filter is proposed in [3], where the battery model parameters are online identified by the forgetting factor recursive least squares algorithm. An adaptive forgetting recursive least squares method is exploited to optimize the estimation alertness and numerical stability [4], so as to achieve online adaption of model parameters. To reduce the iterative computational complexity, a two-stage recursive least squares approach is developed to identify the model parameters [5]; then, the measurement values of the open-circuit voltage at varying relaxation periods and three temperatures are sampled to establish the relationships between SOC and open-circuit voltage. In [6], a multiscale parameter adaptive method based on dual Kalman filters is applied to estimate multiple parameters. Based on the battery circuit model and battery model state equation, the real-time recursive least squares method with forgetting factor is used to identify unknown battery parameters [7]. After introducing the concept of state of health, the average error of the obtained SOC estimation is less than one given value. A novel state and parameter coestimator is developed to concurrently estimate the state and model parameters of a Thevenin model for liquid metal battery [8], where the adaptive unscented Kalman filter (UKF) is employed for state estimation, including a battery SOC. After performing lithium-ion battery modelling and offline parameter identification, a sensitivity analysis experiment is designed to verify which model parameter has the greatest influence on SOC estimation [9]. To improve the SOC estimation accuracy under uncertain measurement noise statistics, a variational Bayesian approximation-based adaptive dual extended Kalman filter is proposed in [10], and the measurement noise variances are simultaneously estimated in the SOC estimation process. To the best of our knowledge, these SOC estimation methodologies can be roughly divided into two kinds, i.e., data-driven methods and model-based methods. In the model-based methods, Kalman filter-based SOC estimation methods have some advantages, such as self-correction, online computation, and complexity reduction. Kalman filter was first proposed to estimate the state of linear systems [12], and then, in order to apply it into nonlinear systems, the extended Kalman filter and unscented Kalman filter were developed [11]. Meanwhile, the data-driven methods typically include the lookup table method, matching learning-based method, artificial neural networks, and support vector machine [13]. The data-driven method means that in estimating the state whatever in linear system or nonlinear system, no mathematical model is needed; i.e., the state is constructed only directly by observed data [14], so a large number of training data covering of all the operating conditions are collected to improve the estimation accuracy of the considered SOC. In this paper, based on above references on SOC estimation for lithium-ion batteries, we also employ unscented Kalman filter to estimate SOC for lithium-ion batteries. First, some priori knowledge about Kalman filter is described to give a detailed introduction. Kalman filter is based on modern filter theory. For the special linear system with Gaussian noise,

Kalman filter is proposed to obtain the minimum mean square estimate about the system state, and this corresponding estimate is named as the optimal filter value. Furthermore, to extend Kalman filter algorithm, the state space model is introduced in the optimal filter theory. The dynamic model and observation model correspond to the state equation and observation equation, respectively; thus, Kalman filter can be extended to deal with the time variant system. Due to its recursive computation iteratively, Kalman filter is easy to implement. However, Kalman filter is suitable under one condition that the considered system is a linear time invariant system with Gaussian white noise, which corresponds to the classical Kalman filter. To relax this strict assumption, unscented Kalman filter algorithm is proposed to solve the state estimation problem for the nonlinear stochastic systems. One core idea of unscented Kalman filter is unscented transformation. The unscented transformation means that the probability density of the considered state can be described by a finite number of sampled points, which can be fully expressed as their means and covariances. After these sampled points are mapped by using state or observation equation, the updated mean and covariance are given through the weighted summation. Generally, the filtering characteristic obtained by our studied unscented Kalman filter is better than that of the classical Kalman filter. Throughout this paper, as SOC of lithium-ion batteries can be reformulated as a state variable in one state space equation, the problem of estimating SOC is changed as a problem of estimating the state variable in this constructed state space equation. Thus, we apply Kalman filter to estimate SOC, corresponding to lithium-ion batteries. Because the state space equation, constructed by physical principle of the lithium-ion battery, coincides with a nonlinear system, one unscented Kalman filter is proposed to study the problem of SOC estimation for a nonlinear system at a series of points, where this nonlinear system corresponds to our state space equation about SOC. When implementing this unscented Kalman filter, the accuracy of SOC estimation is influenced by one designed scaling parameter. Because the choice of scaling parameter may lead to the increased quality of the state estimation, during implementation of unscented Kalman filter, this scaling parameter is always set to be 0 or 1; i.e., the scaling parameter is chosen as one fixed constant. This fixed constant cannot show the merit of the scaling parameter. To give a selection on the scaling parameter, one adjustable selection is proposed to choose the scaling parameter. After one different criterion function is constructed, then the scaling parameter is chosen adaptively by minimizing this established criterion function. The property of this criterion function is shown from its own different observed information and computational complexity. This selection strategy is named as unscented Kalman filter with adjustment scaling parameter. Based on our proposed unscented Kalman filter with adjustment scaling parameter, it is only one single Kalman filter and it is impossible to use only one single filter to describe the state in the whole state space equation. So after inspired by the idea of information fusion theory, we apply our proposed unscented Kalman filter with adjustment scaling parameter on multiple

unscented Kalman filters to obtain their corresponding state estimations. Then, we choose the weighted summation as the final state estimation, whose weights are determined by probability level. Considering these different models, one improved unscented Kalman algorithm based on the iterative multiple models is studied here. Generally, the main contributions of this paper are formulated as follows. (1) For the commonly used unscented Kalman filter, one selection strategy is proposed to choose the scaling parameter adaptively. The optimal scaling parameter is identified through minimizing a maximum likelihood criterion. (2) On the basis of information fusion theory, the idea of iterative multiple models is applied to implement our proposed unscented Kalman filter with adjustment scaling parameter, then the weighted summation from these multiple models is set as the final state estimation, and the weights are determined by probability level. As a consequence, we combine the classical unscented Kalman filter, optimization theory, and information fusion theory to improve the accuracy of the state estimation; then, this state estimation is our considered SOC for the lithium-ion battery.

The paper is organized as follows. In Section 2, the battery modelling is addressed; furthermore, the definition of SOC and the state space models for SOC estimation are also described. Unscented Kalman filter is used to solve the SOC estimation problem for the nonlinear system in Section 3, where the detailed process is also given. In Section 4, one maximum likelihood criterion is constructed to update the scaling parameter adaptively, and the computational complexity of this adjustment is covered. One improved unscented Kalman filter based on iterative multiple models is proposed to consider different models within different sample points in Section 5. In Section 6, two numerical examples illustrate the effectiveness of our proposed unscented Kalman filter with adjustment scaling parameters in estimating the SOC for lithium-ion batteries. Section 7 ends the paper with final conclusion and points out the next topic. A flowchart of our proposed unscented Kalman filter with the adjustment scaling parameter and its other improved multiple models is given in Figure 1, where the yellow parts are our main contributions.

2. Battery Modelling

Our considered lithium-ion battery has some merits in energy density and life, and furthermore, it is the leading development direction of power batteries for electric vehicles in the future. To give a brief introduction on lithium-ion batteries, the internal states of lithium-ion battery are always divided into four parts, i.e., SOC, temperature, rate of current, and state of health. These four states reflect the internal relations of lithium-ion battery with time variable. Here, our emphasis is on the internal structure of lithium-ion battery, which is shown in Figure 2, whose cell generally comprises four parts: a polymer positive electrode, a diaphragm, a negative electrode, and an electrolyte. The positive electrode of the lithium-ion battery is generally composed of lithium-ion polymer. Common cathode lithium-ion polymer materials include lithium phthalate, lithium-ion

phosphate, barium acid strontium, lithium-ion manganate, nickel diamond, and nickel-nickel aluminum ternary lithium. The diaphragm is in the process of the first charge and discharge of the liquid lithium-ion battery. The electrode material reacts with the electrolyte at the solid-liquid phase interface to form a passivation layer covering the surface of the electrode material to isolate the electrode and the electrolyte, and the lithium ion can finish chemical reaction with the diaphragm.

For convenience in the latter simulation example, the lithium battery test needs to charge and discharge the lithium-ion battery at different temperatures and different rates. Therefore, the equipment required for the experimental bench includes a thermostat, a battery charging and discharging device, a ternary neon battery, and a host computer. Lithium battery test platform is plotted in Figure 3, where the detailed processes are described as follows:

Step 1. The charging and discharging positive and negative terminals of the battery are, respectively, connected to the positive and negative electrodes of the battery through the wire harness, and the wire harness of the appropriate diameter is selected according to the allowable charging and discharging ratio of the battery to avoid burning of the wire harness. One end of the voltage-sampling line to the other end of the battery is connected to the voltage sampling and wiring port of the battery charging and discharging device. Finally, the temperature-measuring line of the thermistor is attached to the surface of the battery, and the other side of the temperature-detecting line is connected to the temperature-detecting terminal of the battery charging and discharging device.

Step 2. Set the lithium battery in the incubator, and set the experimental ambient temperature.

Step 3. Start battery charging and discharging equipment and incubator.

Step 4. In the online machine, we edit the charge and discharge test step or import the edited current test file into the host computer to automatically generate the test step; then, set the sampling time and output file save address and start the test.

Actually, in all references on SOC for lithium-ion battery, two commonly used battery models exist, i.e., equivalent circuit model and electrochemical model. As the electrochemical model is very complex, and it is very difficult to design the latter Kalman filter in case of this electrochemical model, so here in modelling the lithium-ion battery, the equivalent circuit model is recently used. The equivalent circuit model regards the battery internal reactions as a circuit, containing some electronic components, so the equivalent circuit model consists of basic circuit components such as resistors, capacitors, and voltage sources. These four basic circuit components are widely explored, due to their relatively simple mathematical structure and reduced computational complexity. Equivalent circuit model is shown in Figure 4, which is simple and clear in physical meaning, and will be applied to describe the battery

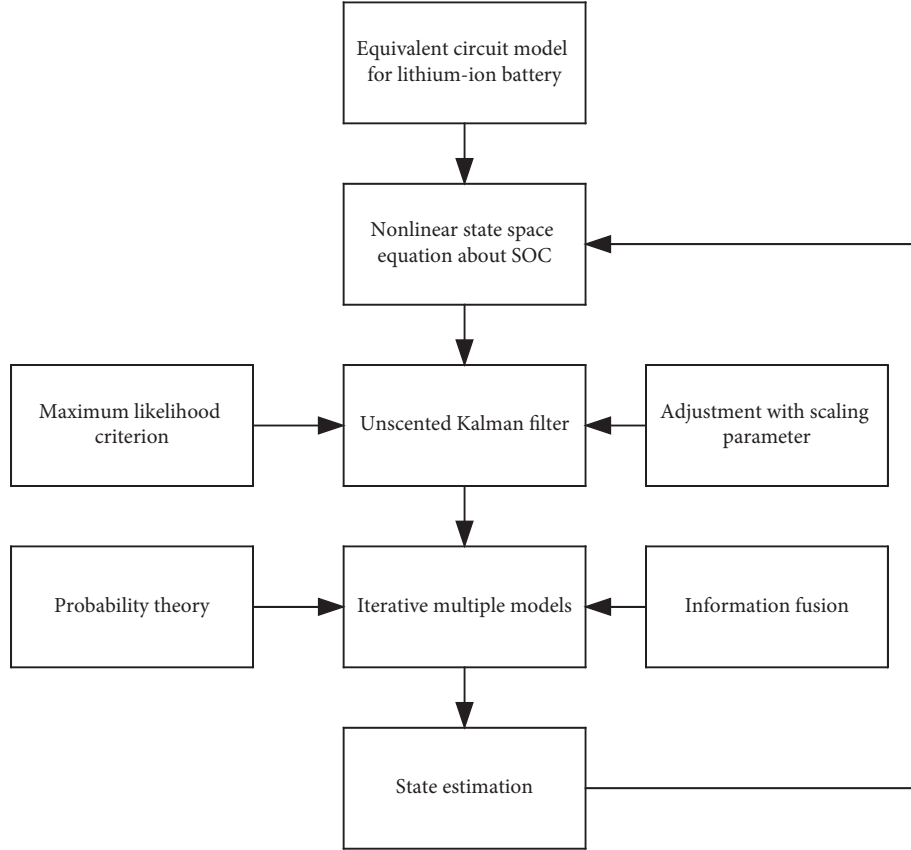


FIGURE 1: A flowchart of our paper.

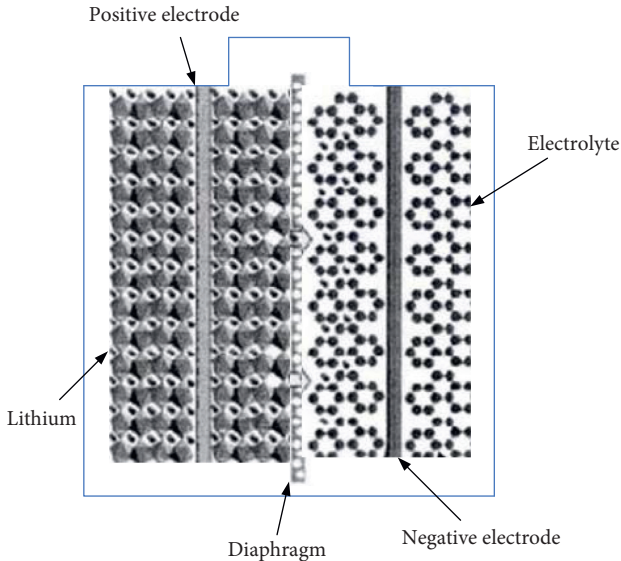


FIGURE 2: Battery internal structure.

charging and discharging properties. Through balancing the tradeoff between model accuracy and computational complexity, one Thevenin equivalent circuit model is chosen for a Li-ion battery, which is regarded as our battery model.

Using Kirchhoff law or some physical principles, define variable U_{load} as follows:

$$U_{\text{load}} = U_{\text{OC}} - IR_0 - U_p, \quad (1)$$

$$I = \frac{U_p}{R_p} + C_p \frac{dU_p}{dt}, \quad (2)$$

where U_{load} is the terminal voltage, I is the load current, R_0 is the internal ohmic resistance, R_p and C_p are the polarization resistance and polarization capacitance of the battery, U_p is the polarization voltage, and U_{OC} is the open-circuit voltage, which is monotonic with SOC. Furthermore, U_{OC} can be rewritten as the following polynomial form:

$$U_{\text{OC}}(x) = d_5 + d_4x + d_3x^2 + d_2x^3 + d_1x^4, \quad (3)$$

where $\{d_i\}_{i=1}^5$ are the coefficients of polynomial form (3) and x is the SOC of lithium-ion battery. SOC is defined as a ratio of the remaining capacity over the rated capacity. Furthermore, from equation (3), as the voltage is in polynomial form, in order to simplify the later mathematical analysis, we assume the charging and uncharging have the same behavior. Using the ampere hour counting principle, SOC can be expressed as follows:

$$\text{SOC}(t) = \text{SOC}(t_0) - \eta \int_{t_0}^t \frac{Idt}{Q_N}, \quad (4)$$

where t is the sample time, $\text{SOC}(t)$ is the SOC of lithium-ion battery at time instant t , $\text{SOC}(t_0)$ is the initial SOC, I is the load current, η is the coulombic efficiency, and Q_N is the

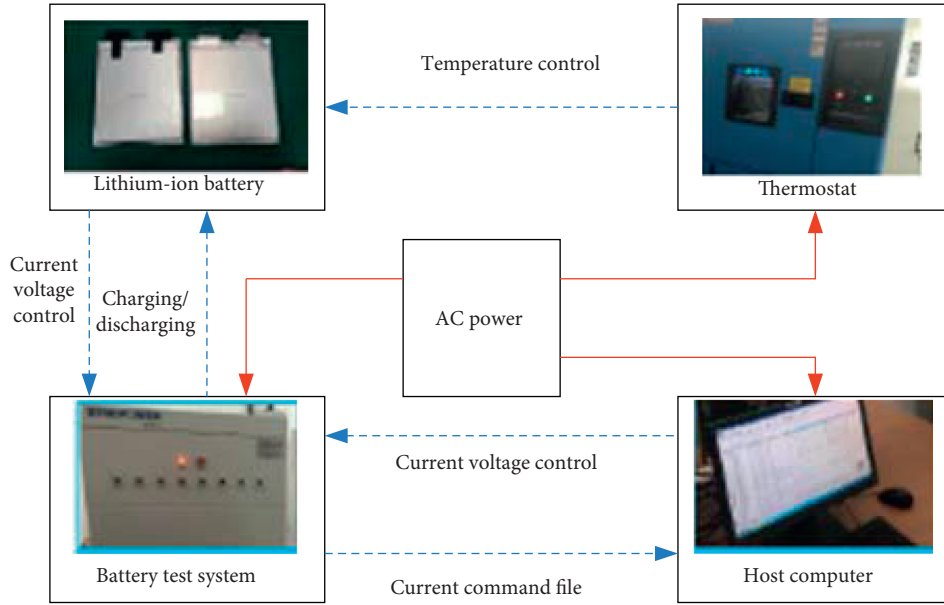


FIGURE 3: Lithium battery test platform.

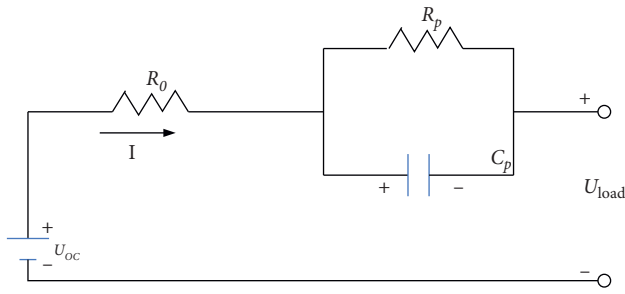


FIGURE 4: Equivalent circuit model.

nominal capacity of battery. State space equation can be obtained by discretization, and then, we obtain the following discrete state space equation:

$$\begin{bmatrix} \text{SOC}_k \\ U_{p,k} \end{bmatrix} = \begin{bmatrix} 1 & 0 \\ 0 & \exp\left(-\frac{T_s}{R_p C_p}\right) \end{bmatrix} \begin{bmatrix} \text{SOC}_{k-1} \\ U_{p,k-1} \end{bmatrix} + \begin{bmatrix} -\eta \\ R_p \left(1 - \exp\left(-\frac{T_s}{R_p C_p}\right)\right) \end{bmatrix} I_{k-1}, \quad (5)$$

$$U_{\text{load},k} = U_{\text{OC}}(\text{SOC}_k) - U_{p,k} - I_k R_0, \quad (6)$$

where k is the sample time, SOC_k is the state value at the k th sample time, and T_s is the specified small sampling period. $U_{\text{OC}}(\text{SOC}_k)$ denotes a nonlinear function of SOC_k . The parameters in above each matrix of state space equations (5) and (6) can be identified by the classical least squares method, but our goal in this paper is to estimate SOC (SOC_k) at time instant k by using Kalman filter.

3. Unscented Kalman Filter for SOC Estimation

In this section, we start to apply unscented Kalman filter algorithm (UKF) to estimate SOC. By combining equations (5) and (6), SOC_k at time instant k is one state variable in that state space equation. Furthermore, we want to testify which parameter will influence SOC estimation; then, this parameter will be added as the new state variables in the extended state space equation.

3.1. Preliminary. As the main model parameter R_0 is classified as a new state variable with U_p and SOC; then, an extended state space equation for UKF can be given as follows:

$$\begin{bmatrix} \text{SOC}_k \\ U_{p,k} \\ R_{0,k} \end{bmatrix} = \begin{bmatrix} 1 & 0 & 0 \\ 0 & \exp\left(-\frac{T_s}{R_p C_p}\right) & 0 \\ 0 & 0 & 1 \end{bmatrix} \begin{bmatrix} \text{SOC}_{k-1} \\ U_{p,k-1} \\ R_{0,k-1} \end{bmatrix} + \begin{bmatrix} -\eta \\ R_p \left(1 - \exp\left(-\frac{T_s}{R_p C_p}\right)\right) \\ 0 \end{bmatrix} I_{k-1} + \begin{bmatrix} w_{1,k-1} \\ w_{2,k-1} \\ w_{3,k-1} \end{bmatrix}, \quad (7)$$

$$U_{\text{load},k} = U_{\text{OC}}(\text{SOC}_k) - U_{p,k} - I_k R_0 + v_k. \quad (8)$$

To apply UKF into the above state space equation to estimate the first state variable, we rewrite equations (7) and (8) as follows:

$$\begin{cases} x_{k+1} = f_k(x_k) + w_k, \\ z_k = h_k(x_k) + v_k, \quad k = 0, 1, 2, \dots, \end{cases} \quad (9)$$

where

$$\begin{aligned} x_{k+1} &= \begin{bmatrix} \text{SOC}_{k+1} \\ U_{p,k+1} \\ R_{0,k+1} \end{bmatrix}, \\ f_k(x_k) &= \begin{bmatrix} 1 & 0 & 0 \\ 0 & \exp\left(\frac{T_s}{R_p C_p}\right) & 0 \\ 0 & 0 & 1 \end{bmatrix} \begin{bmatrix} \text{SOC}_k \\ U_{p,k} \\ R_{0,k} \end{bmatrix} \\ &+ \begin{bmatrix} -\eta \\ R_p \left(1 - \exp\left(\frac{T_s}{R_p C_p}\right)\right) \\ 0 \end{bmatrix} I_k, \\ w_k &= \begin{bmatrix} w_{1,k} \\ w_{2,k} \\ w_{3,k} \end{bmatrix}, \\ z_k &= U_{\text{load},k}, \\ h_k(x_k) &= U_{\text{OC}}(\text{SOC}_k) - U_{p,k} - I_k R_0, \end{aligned} \quad (10)$$

where in equation (9), $x_k \in R^{n_x}$ and $z_k \in R^{n_z}$ denote the state vector and measurement vector at time instant k , respectively. Two maps $f_k: R^{n_x} \rightarrow R^{n_x}$ and $g_k: R^{n_x} \rightarrow R^{n_z}$ denote two unknown nonlinear functions, and $w_k \in R^{n_x}$ and $v_k \in R^{n_z}$ are two state and measurement noises with zero mean. These white noises are independent and identically distributed between each other, and their covariance matrices are Σ_w and Σ_v . x_0 is the initial state, and its mean and covariance matrix are \bar{x}_0 and P_0 , respectively. The initial state x_0 is independent of these two white noises w_k and v_k .

3.2. Unscented Kalman Filter Algorithm. After observing equation (9), our goal is to infer the state estimation from observed data; it corresponds to the filter process for that nonlinear stochastic system. In the framework of Bayesian theory, state estimation is equivalent to complete our approximation of the posterior probability distribution of the state vector, in case of the observed data. It is well known that this posterior probability distribution is named as the

conditional probability density function on the basis of the observed data. Our unscented Kalman filter algorithm in Bayesian nonlinear filtering is to obtain a series of points in state space form and to match the Gaussian distribution in each update step. State estimation depends on minimizing one given criterion function, for example, the commonly used minimum square error criterion:

$$J_k = E[(x_k - \hat{x}_k)(x_k - \hat{x}_k)^T | Z^k], \quad (11)$$

where E is the expectation and Z^k is the set of all observed data to time instant k , i.e.,

$$Z^k = [z_0, z_1, \dots, z_k]^T, \quad (12)$$

In equation (11), \hat{x}_k is the state estimation of state x_k and \hat{x}_k is a function of Z^k . After minimizing criterion function (11), state estimation \hat{x}_k is obtained as follows:

$$\hat{x}_k = \hat{x}_{k|k} = E[x_k | Z^k], \quad (13)$$

where equation (13) is the conditional mean and its expectation can be approximated by stochastic sample strategy. For the linear system, this conditional mean is simplified to the classical Kalman filter algorithm. But on the contrary, in the nonlinear system, it is difficult to compute the expectation operation. Unscented Kalman filter algorithm calculates the mean and covariance matrix on the filtering and prediction process iteratively. Set

$$x^{a,b} = [x^a, x^{a+1}, \dots, x^b]^T, \quad (14)$$

and $I_{a \times b}$ and $0_{a \times b}$ are the diagonal matrix and zero matrix with dimension $a \times b$. Factorize the matrix P as follows:

$$P = \sqrt{P} \sqrt{P}^T. \quad (15)$$

Then, the detailed unscented Kalman filter algorithm can be formulated as follows:

Step 1 (initialization): set time instant $k = 0$ and define the predictive mean and covariance matrix in case of prior initial condition:

$$\begin{cases} \hat{x}_{0|-1} = E[x_0] = \bar{x}_0, \\ P_{0|-1}^x = \text{cov}[x_0] = P_0^x. \end{cases} \quad (16)$$

Step 2 (filtering): compute a series of points σ as $\{x_{k|k-1}^i\}_{i=0}^{2n_x}$ and their corresponding weights $\{w_{k|k-1}^i\}_{i=0}^{2n_x}$ as follows:

$$x_{k|k-1}^{0:2n_x} = \hat{x}_{k|k-1} I_{1 \times b} + c \left[0_{n_x \times 1} \sqrt{P_{k|k-1}^x} - \sqrt{P_{k|k-1}^x} \right], \quad (17)$$

$$w_{k|k-1}^{0:2n_x} = \frac{1}{n_x + \mu} \left[\mu \frac{1}{2} \cdots \frac{1}{2} \right],$$

where $b = 2n_x + 1$ is the total number of points σ and $c = \sqrt{n_x + \mu}$, μ is the scaling parameter. At each point σ ,

the transformation is obtained through nonlinear function h_k :

$$z_{k|k-1}^i = h_k(x_{k|k-1}^i), \quad \forall i. \quad (18)$$

Compute the following second-order moment for approximating the prediction value as follows:

$$\begin{aligned} \hat{z}_{k|k-1} &= \sum_{i=0}^{2n_x} w_{k|k-1}^i z_{k|k-1}^i, \\ P_{k|k-1}^z &= \sum_{i=0}^{2n_x} w_{k|k-1}^i (z_{k|k-1}^i - \hat{z}_{k|k-1}) (z_{k|k-1}^i - \hat{z}_{k|k-1})^T + \sum_k^v, \\ P_{k|k-1}^{xz} &= \sum_{i=0}^{2n_x} w_{k|k-1}^i (x_{k|k-1}^i - \hat{x}_{k|k-1}) (z_{k|k-1}^i - \hat{z}_{k|k-1})^T. \end{aligned} \quad (19)$$

The estimations for the mean and covariance matrix are as follows:

$$\begin{aligned} \hat{x}_{k|k} &= \hat{x}_{k|k-1} + K_k (z_k - \hat{z}_{k|k-1}), \\ P_{k|k}^x &= P_{k|k-1}^x - K_k P_{k|k}^z K_k^T, \end{aligned} \quad (20)$$

where the filtering gain K_k is defined as

$$K_k = P_{k|k-1}^{xz} (P_{k|k-1}^z)^{-1}. \quad (21)$$

Step 3 (prediction): compute a series of points σ as $\{x_{k|k}^i\}_{i=0}^{2n_x}$ and their corresponding weights $\{w_{k|k}^i\}_{i=0}^{2n_x}$ are

$$\begin{aligned} x_{k|k}^{0:2n_x} &= \hat{x}_{k|k} I_{1 \times b} + c \left[0_{n_x \times 1} P_{k|k}^x - \sqrt{P_{k|k}^x} \right], \\ w_{k|k}^{0:2n_x} &= \frac{1}{n_x + \mu} \left[\mu \frac{1}{2} \cdots \frac{1}{2} \right]. \end{aligned} \quad (22)$$

Furthermore, at each point σ , after nonlinear function f_k is applied to transform, we obtain

$$\bar{x}_{k+1|k}^i = f_k(x_{k|k}^i), \quad \forall i. \quad (23)$$

Compute the following second-order moment for the state as follows:

$$\begin{aligned} \hat{x}_{k+1|k} &= \sum_{i=0}^{2n_x} w_{k|k}^i \bar{x}_{k+1|k}^i, \\ P_{k+1|k}^x &= \sum_{i=0}^{2n_x} w_{k|k}^i (\bar{x}_{k+1|k}^i - \hat{x}_{k+1|k}) (\bar{x}_{k+1|k}^i - \hat{x}_{k+1|k})^T + \sum_k^w. \end{aligned} \quad (24)$$

Set $k = k + 1$, and continue to step 2.

After the unscented transformation, the position of point σ is determined by the mean and covariance matrix of one transformed variable. Then, the position of point σ will affect the denominator of the covariance matrix and the scaling parameter. More specifically, in the predictive step, the position of point σ is chosen in the control of one super ellipsoid, where $\hat{x}_{k|k}$ is one interior point. As the primary transformation direction $\hat{x}_{k|k}$ is given by one feature vector of that covariance matrix $P_{k|k}^x$, in the filtering step, the primary transformation direction at $\hat{x}_{k|k-1}$ is determined by one feature vector of that covariance matrix $P_{k|k-1}^x$. The size of super ellipsoid is judged by the scaling parameter and the position of point σ simultaneously. The scaling parameter μ may affect the accuracy, and it is always set as $\mu = 3 - n_x$. The choice of this scaling parameter can be achieved by series expansion error, and this series expansion error represents the difference between the true mean and its unscented transformation approximation. The first three terms of the series expansion will be zero through the approximate selection of the weights, and the fourth term can also be guaranteed to be zero on the basis of the scaling parameter. Moreover, the determination of the scaling parameter is related with the criterion function. But in the unscented transformation of our considered unscented Kalman filter algorithm, no fixed scaling parameter is given to ensure high accuracy of the state estimation. The position of the working point or the expected state of the target will change with the time invariant system. For this reason, one optimization strategy based on minimizing the approximate maximum likelihood function is applied to adjust the scaling parameter adaptively.

4. Adjustment of Scaling Parameter

The choice of scaling parameter depends on one criterion function with some estimation in unscented transformation. But in our above state estimation for unscented Kalman filter algorithm, no true variables can be acquired. The only information available for state estimation is the sequence of observations. This limitation emphasizes the importance of adjusting the scaling parameter adaptively. In this section, the maximum likelihood criterion is proposed to obtain one suitable scaling parameter. From the theoretical perspective, the maximum likelihood criterion coincides with the probability density function within the unscented Kalman filter algorithm, so the maximum likelihood criterion requires a prior knowledge about the state and two probability density functions $p(w_k)$ and $p(v_k)$ of the observed noises. When the maximum likelihood criterion is used to design the optimal scaling parameter μ_1^k , its explicit form is given as

$$\mu_1^k = \arg \min_{\mu} p(z_k | Z^{k-1}, \mu). \quad (25)$$

If two probability density functions $p(x_k | Z^{k-1})$ and $p(z_k | x_k) = p_{w_k}(z_k - h_k(x_k))$ are all Gaussian distributions, then we have

$$p(z_k | Z^{k-1}, \mu) = N(\hat{z}_{k|k-1}(\mu), P_{k|k-1}^z(\mu)), \quad (26)$$

where $N(\hat{z}_{k|k-1}(\mu), P_{k|k-1}^z(\mu))$ is one Gaussian normal distribution with mean $\hat{z}_{k|k-1}(\mu)$ and covariance matrix

$P_{k|k-1}^z(\mu)$ and the mean and covariance matrix are all functions of the scaling parameter μ . To obtain one closed and analytic solution for equation (16), some numerical optimization methods can be applied to achieve the goal, for example, numerical grid method or global adaptive method. The numerical grid method covers a feasible optimization area $[\mu_{\min}, \mu_{\max}]$, and then, μ is obtained by equal space mesh point. After the optimization function is calculated at the equal space grid, the optimal scaling parameter μ^* is chosen by selecting the maximum or minimum grid point. In the global adaptive random search algorithm, the minimum value of the scaling parameter is set as the lower bound of the adaptive interval, i.e., $\mu_{\min} = 0$. This value guarantees that the covariance matrix of the random variable in unscented Kalman filter process is a positive form. The upper bound μ_{\max} of the adaptive interval can be set as one probability level; it means that the probability level of the stochastic variable x lies in one region as follows:

$$P^* = \frac{2^{1-(n_x/2)}}{\Gamma(n_x/2)} \int_0^{\sqrt{n_x + \mu_{\max}}} e^{-(t^2/2)} t^{n_x-1} dt, \quad (27)$$

where P^* is the designed parameter and $\Gamma(n_x/2)$ is the Gram function. When dimension n_x is a special case, $n_x = 2$; then, μ_{\max} is chosen as

$$\mu_{\max} = -2 \log(1 - P^*) - 2. \quad (28)$$

If we set $P^* = 0.999$, then $\mu_{\max} = 11.8$. But this global adaptive process for choosing the optimal scaling parameter will increase the computational complexity for unscented Kalman filter algorithm. This adaptive adjustment of scaling parameter can be applied to all time instants, instead of being limited to nonlinear function $h_k(x_k)$ of state estimation $\hat{x}_{k|k-1}$. And for the special case of linear function $h_k(x_k)$, the scaling parameter does not give any performance improvement for the unscented transformation, but the computational complexity can be greatly reduced. Generally, the adjustment for the scaling parameter in the unscented Kalman filter algorithm is formulated as follows, where the maximum likelihood criterion is used here:

Step 1 (initialization): set $\mu_{\min} = 0$ and compute μ_{\max} from equation (20); define the nonlinear measurement threshold as T and the initial time instant $k = 0$. The mean and covariance matrix at initial condition are defined as

$$\begin{cases} \hat{x}_{0|-1} = E[x_0] = \bar{x}_0, \\ P_{0|-1}^x = \text{cov}[x_0] = P_0^x. \end{cases} \quad (29)$$

Step 2 (adjustment): define the scaling parameter as follows:

$$\mu_k = \begin{cases} \mu_k^3, & \text{if } \lambda_{\max}(z^T P_{k|k-1} z) > T, \\ 3 - n_x, & \text{otherwise.} \end{cases} \quad (30)$$

Step 3 (filtering): implement the filtering step in the unscented Kalman filter algorithm and substitute the optimal scaling parameter μ_k into step 2.

Step 4 (prediction): implement the prediction step in the unscented Kalman filter algorithm and substitute the optimal scaling parameter μ_k into step 2.

Then, set $k = k + 1$, continue the above steps, and turn to step 2.

5. One Improved Unscented Kalman Filter

To extend the abovementioned unscented Kalman filter, we find that it is impossible to use only one model to describe the state estimation in only one simple filter. In this section, different models would be applied in different filters, and one improved unscented Kalman filter is studied based on iterative multiple models. The basic idea of multiple models is explained first. The possible motion mode of the target is mapped into one model set; then, each model in this model set indicates different modes. Through some multiple filters based on different modes in parallel, the final state estimation of the output will be chosen as the fusion result, corresponding to the local state estimation from each filter. Each filter corresponds to its own state space model, while different state space models describe different motion modes, so the state estimation, coming from each filter, is also different. Roughly speaking, iterative multiple model algorithm assigns different weights to different estimation, and these different weights are determined by probability level. The improved unscented Kalman filter is plotted in Figure 5. This recursive algorithm includes four steps, i.e., initialization, conditional filter, probability update, and combined output.

Let $M_k^{(t)}$ signifies the effective event at the t th sampled period for model $M^{(t)}$; then, $M_{k-1}^{(j)}$ is the effective event at the $k-1$ th sampled period for model $M^{(j)}$. For the case of r models, the improved unscented Kalman filter algorithm based on iterative multiple models is formulated as follows:

- (1) Apply the estimation $\hat{x}^{(j)}(k-1|k-1)$ of model j and covariance matrix $P^{(j)}(k-1|k-1)$ to compute the hybrid initialization, matching to model $M^{(t)}$. Assume that the considered models satisfy the Markov property, then

$$\hat{x}^{(t)}(k-1|k-1) = \sum_{j=1}^r \hat{x}^{(j)}(k-1|k-1) \mu^{(j|t)}(k-1|k-1),$$

$$\begin{aligned} P^{(t)}(k-1|k-1) &= \sum_{j=1}^r P^{(j)}(k-1|k-1) + ((\hat{x}^{(j)}(k-1|k-1) \\ &\quad - 1) \hat{x}^{(t)}(k-1|k-1)) \mu^{(j|t)} \\ &\quad \cdot (k-1|k-1), \end{aligned}$$

$$\mu^{(j|t)}(k-1|k-1) = p(M^{(j|t)}(k-1) | M^{(t)}(k), Z_{k-1})$$

$$= \frac{1}{\bar{c}_t} \pi_{jt} \mu^{(j)}(k-1),$$

(31)

where $\mu^{(j)}(k-1)$ is the probability level for model $M^{(j)}$, $\bar{c}_t = \sum_{j=1}^r \pi_{jt} \mu^{(j)}(k-1)$ is one constant, and

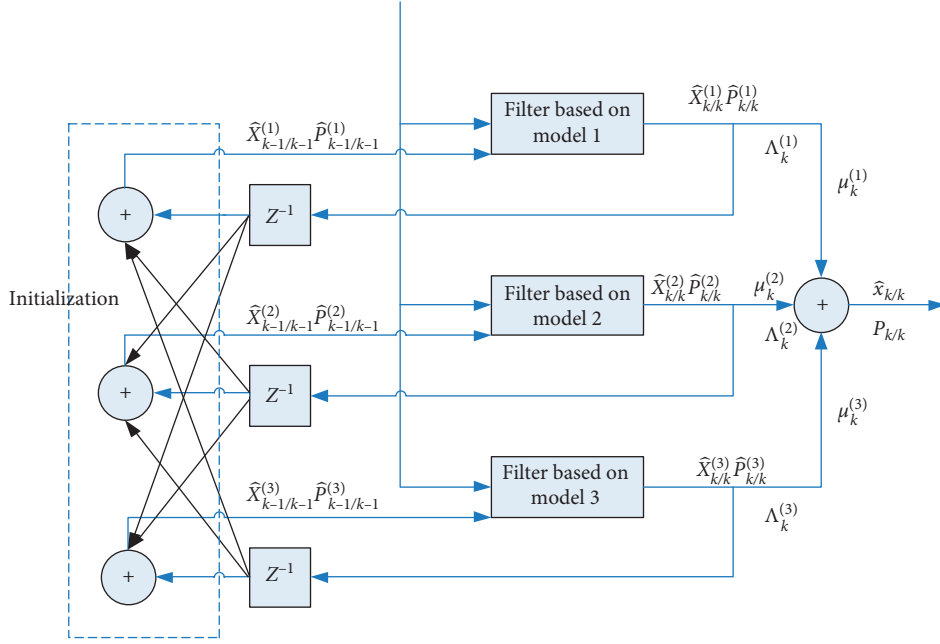


FIGURE 5: Improved Kalman filter.

$\mu^{(j)}$ is the transition probability from model $M^{(j)}$ to model $M^{(t)}$.

- (2) Unscented Kalman filter on each model: unscented Kalman filter is used in $\hat{x}^{(t)}(k-1|k-1)$ and $P^{(t)}(k-1|k-1)$ for all models $t = 1, 2, \dots, r$. Without loss of generality, the above adjustment of scaling parameter is also used here.

(a) Initialization: apply $\hat{x}^{(t)}(k-1|k-1)$ and $P^{(t)}(k-1|k-1)$ to solve many sigma points $\{x_i^{(t)}\}$ and weights $\{w_i^{(t)}\}$.

(b) Sigma points: use each state model to predict state estimations $\{x_i^{(t)}(k|k-1)\}$ and sigma points $\{Z_i^{(t)}(k)\}$ and then compute some prediction values $\{\hat{x}^{(t)}(k|k-1)\}$ and $\{Z^{(t)}(k)\}$. Covariance matrix: apply $\{\hat{x}^{(t)}(k|k-1)\}$, $\{Z^{(t)}(k)\}$, and $\{w_i^{(t)}\}$ to compute the covariance matrix $P^{(t)}(k|k-1)$, cross covariance matrix $P_{xz}^{(t)}(k)$, and information covariance matrix $S^{(t)}(k)$.

(c) Updated strategy: the filtering gain is as follows:

$$K^{(t)} = \frac{P_{xz}^{(t)}(k)}{S^{(t)}(k) + R(k)}. \quad (32)$$

$$x^{(t)}(k|k) = x^{(t)}(k|k-1) + K^{(t)}(z(k) - z^{(t)}(k)). \quad (33)$$

$$P^{(t)}(k|k) = P^{(t)}(k|k-1) + K^{(t)}\{S^{(t)}(k) + R(k)\}(K^{(t)})^T. \quad (34)$$

- (3) Model probability updated is

$$\begin{aligned} \Lambda^{(t)}(k) &= p(Z(k) | M^{(t)}(k), Z_{k-1}) = p(\bar{Z}^{(t)}(k) | M^{(t)}(k), Z_{k-1}) \\ &= |2\pi S^{(t)}(k)|^{-(1/2)} \times \exp\left\{-\frac{1}{2}(\bar{Z}^{(t)}(k))^T (S^{(t)}(k))^{-1} \cdot (\bar{Z}^{(t)}(k))\right\}, \end{aligned}$$

$$\mu^{(t)}(k) = P(M^{(t)}(k) | Z^k) = \frac{1}{c} \Lambda^{(t)}(k) \bar{c}_t, \quad (35)$$

where $\Lambda^{(t)}(k)$ is the likelihood function for filter, and

$$\begin{aligned} \bar{Z}^{(t)}(k) &= Z(k) - Z^{(t)}(k), \\ \bar{c}_t &= \sum_{j=1}^r \pi_{jt} \mu^{(j)}(k-1), \\ c &= \sum_{j=1}^r \Lambda^{(j)}(k) \bar{c}_j. \end{aligned} \quad (36)$$

- (4) State estimation fusion is

$$\begin{aligned} \hat{X}(k|k) &= \sum_{i=1}^r X^{(i)}(k|k) \mu^{(i)}(k), \\ P(k|k) &= \sum_{i=1}^r P^{(i)}(k|k) + \left(\hat{X}(k|k) - \hat{X}^{(i)}(k|k)\right) \\ &\quad \times \left(\hat{X}(k|k) - \hat{X}^{(i)}(k|k)\right)^T \mu^{(i)}(k). \end{aligned} \quad (37)$$

The updated state is as follows:

The updated covariance matrix is as follows:

After introducing the adaptive adjustment process of the scale parameter into unscented Kalman filter algorithm, better tracking performance can be obtained than the classical Kalman filter. The mission of the improved unscented Kalman filter with iterative multiple models is to extend the tracking problem for multiobjections.

6. Simulation Examples

Here, in this section, two simulation examples are given to prove the efficiency of this unscented Kalman filter with adjustment scaling parameter for tracking one ground target and SOC estimation for lithium-ion battery, respectively.

6.1. First Simulation Example. In the first simulation example, our goal is to track one continuous time acceleration motion model with white noise. The state of this ground target is defined as follows:

$$x_k = [x_{1k}, x_{2k}, x_{3k}, x_{4k}]^T = [x_k, y_k, \dot{x}_k, \dot{y}_k]^T, \quad (38)$$

where the above target state contains the position and velocity in the x direction and y direction, respectively, and the dimension is $n_x = 4$. Then, the motion equation is

$$\begin{aligned} x_{k+1} &= Fx_k + Gw_k, \\ F &= \begin{bmatrix} 1 & 0 & T & 0 \\ 0 & 1 & 0 & T \\ 0 & 0 & 1 & 0 \\ 0 & 0 & 0 & 0 \end{bmatrix}, \\ G &= \begin{bmatrix} 0.5T^2 & 0 \\ 0 & 0.5T^2 \\ T & 0 \\ 0 & T \end{bmatrix}, \end{aligned} \quad (39)$$

where $T = 1$ s is the sampled interval, w_k is the state noise with Gaussian zero mean, and its covariance matrix is Σ_k^w , i.e.,

$$\begin{aligned} P(w_k) &= N\left(0, \sum_k^w\right), \\ \sum_k^w &= 9.9 \times 10^{-2} I_2. \end{aligned} \quad (40)$$

The ground target is observed by using a radar detector, and the observation z_k at time instant k from the radar detection is the angle between the ground target and the radar detection. When the radar detector is on $[x_k^0, y_k^0]$ at time instant k , then the observation z_k at time instant k is as follows:

$$\begin{cases} z_k = \arctan \frac{x_k - x_k^0}{y_k - y_k^0} + v_k, \\ \sum_k^v = 1. \end{cases} \quad (41)$$

This ground target is 10 km away from the radar detector with angle -135° and constant velocity 15 m/s. Define the initial position of the ground target is $[7, 7]$, and the original position of

the radar detector is set to be the origin $[0, 0]$. In the whole unscented Kalman filter algorithm with adjustable scaling parameter, the initial probability density of the filter is chosen as

$$P(r) = N(\sqrt{7^2 + 7^2}, 16). \quad (42)$$

The probability density of the velocity is

$$P(s) = N(\bar{s}, 16). \quad (43)$$

The largest scaling parameter is set as $\mu_{\max} = 14$, and then we obtain that $P^* = 0.999$. The number of grids used to cover the entire interval is $N_\mu = 20$. Then, the performance corresponding to our considered filter is measured by one mean square error root, which is defined as follows:

$$\text{RMS}_\mu = \frac{1}{M} \sum_{i=1}^M \left[(\hat{x}_k(i) - x_k(i))^2 + (\hat{y}_k(i) - y_k(i))^2 \right]^{1/2}. \quad (44)$$

To show the closed relations between mean square error roots and different signal-to-noise ratios, we do some simulations on model (39) and (41), where we take three cases as follows: low signal-to-noise ratio $\Sigma_k^v = (5^\circ)^2$; mean signal-to-noise ratio $\Sigma_k^v = (2^\circ)^2$; and high signal-to-noise ratio $\Sigma_k^v = (0.07)^\circ^2$. The relationship between the performance of the target state estimation and the threshold value in the unscented Kalman filter algorithm is shown in Figure 6, where three curves are represented as the above three cases. From Figure 6, we see that the adjustment of the scaling parameter adaptably does not make any improvement on high signal-to-noise ratio, but instead great improvements for low and medium signal-to-noise ratios.

In Figure 6, in case of the high signal-to-noise ratio, the effect from the scaling parameter on the state estimation is less. This is the reason why the scaling parameter does not make any improvement on high signal-to-noise ratio. But on the contrary, for low and medium signal-to-noise ratios, the scaling parameter is one important factor, affecting the estimation accuracy.

6.2. Second Simulation Example. The second simulation example is concentrated on SOC estimation for lithium-ion batteries. Here, we do not yet have the experimental platform, so this second simulation example is based on references in the open references. To acquire experimental data such as current, voltage, and temperature from the battery, a battery test bench was established. The configuration of the battery test bench is shown in Figure 3.

Based on the experimental platform, the open-circuit voltage of the battery has a monotonic relationship with the SOC. The relation between open-circuit voltage and SOC is established by running test on the considered lithium-ion battery. Let all batteries be fully charged and rested for 3 hours, such that the internal chemical reactions attain a desired equilibrium state. Moreover, the discharge test includes a sequence of pulse current of 1 C with 6-min discharge and 10-min rest; then, the discharge test can make the battery to return back to its expected equilibrium state before running the next cycle. As three parameters are incorporated into the state variables simultaneously using the extended dimension

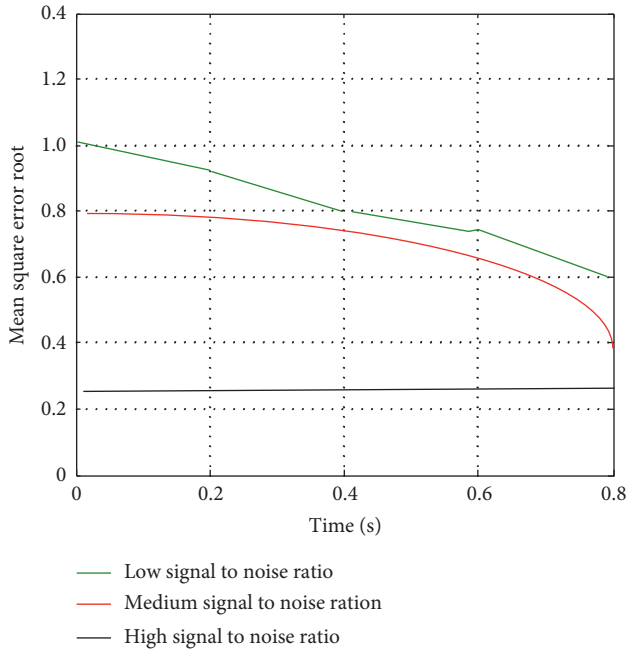


FIGURE 6: Relations between mean square error root and signal-to-noise ratio.

method, so first we analyse the sensitivity analysis for the model parameter R_0 , shown in Figure 7. The test range for R_0 must take abnormal range conditions into account. Taking the existence of extreme conditions and all types of noise into account, it is necessary to increase to 20%. After a complete SOC estimation of the target sample, the average for the absolute error is calculated. A complete SOC estimation process is recorded as a step, recording the step with k . The sensitivity analysis process for R_p and C_p is similar to that of R_0 . The sensitivity analysis for R_p and C_p is shown in Figures 8 and 9, which show that the sensitivity of R_p and C_p and R_0 decreases in turn. Also from these three figures, we see that the response of the considered state space system depends more on two parameters R_0 and R_p , as their sensitivity curves are growing with time or iterative step.

U_{OC} is rewritten as the following polynomial form $U_{OC}(x) = d_5 + d_4x + d_3x^2 + d_2x^3 + d_1x^4$. To identify these unknown parameters in this polynomial form, the least squares method is used to achieve this goal. Then, the identification result for this polynomial form is given in Figure 10, which shows the relation between the true data point and its identified polynomial form.

In whole simulation process, the true parameters can be identified by using some system identification strategies, for example, least squares method, instrumental variable method, and maximum likelihood method. Then, identified parameters are obtained as follows:

$$\begin{aligned}
 R_0 &= 0.0994 \Omega, \\
 R_p &= 0.030 \Omega, \\
 C_p &= 2.773 \text{ KF}, \\
 I &= 1.10 \text{ A}, \\
 T_s &= 0.3 \text{ S}.
 \end{aligned}
 \tag{45}$$

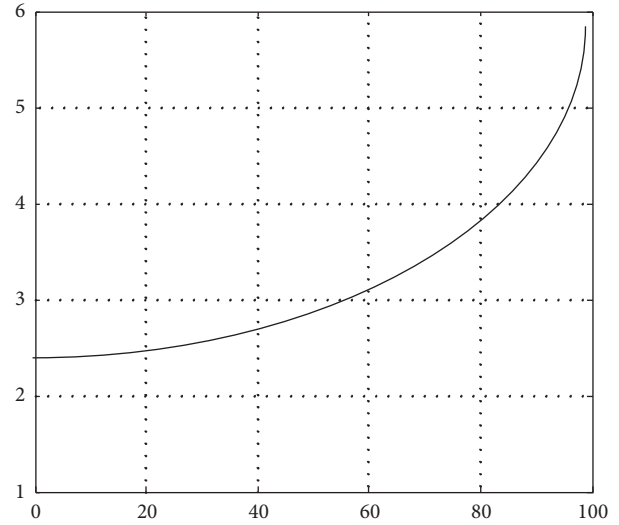


FIGURE 7: Sensitivity analysis of R_0 .

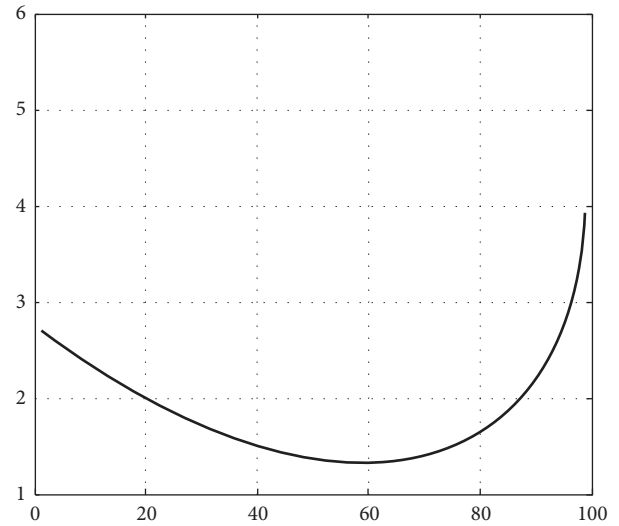


FIGURE 8: Sensitivity analysis of R_p .

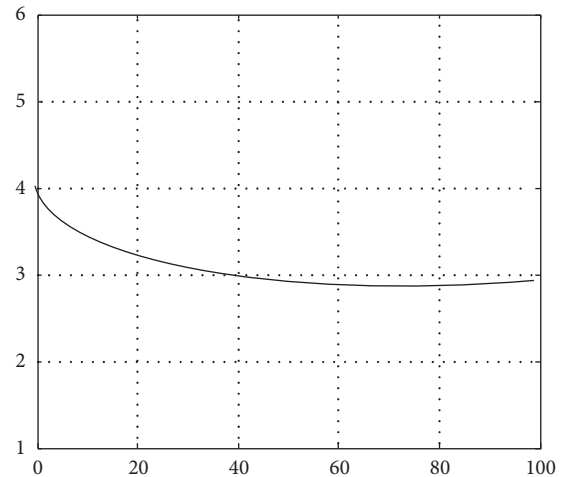


FIGURE 9: Sensitivity analysis of C_p .

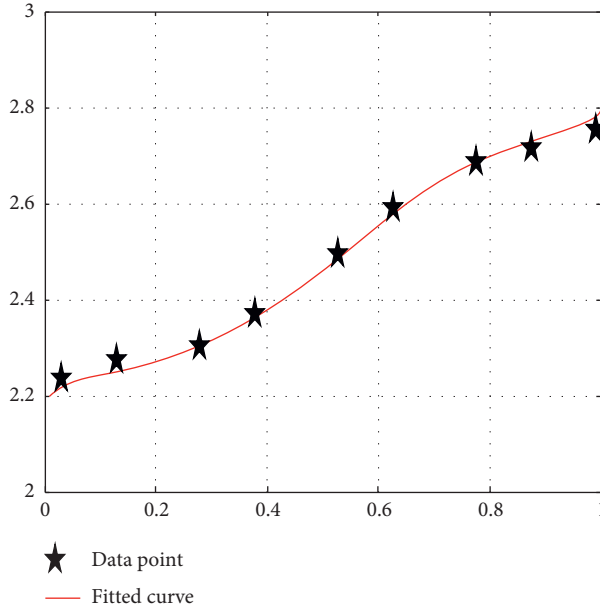


FIGURE 10: Polynomial form for $U_{OC}(x)$.

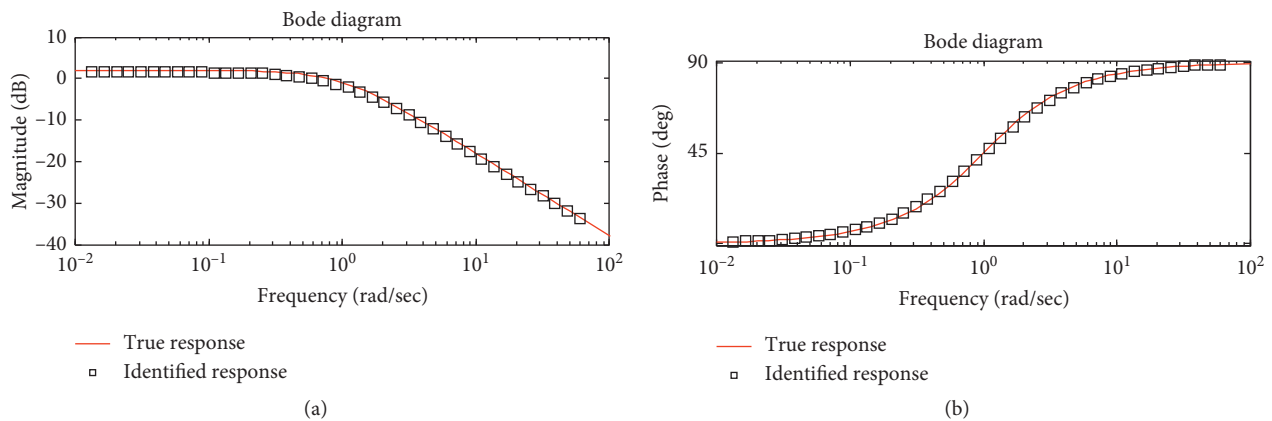


FIGURE 11: Comparison of the system responses.

Then, these three matrices are obtained as follows:

$$\begin{aligned}
 A &= \begin{bmatrix} 1 & 0 & 0 \\ 0 & 0.68 & 0 \\ 0 & 0 & 1 \end{bmatrix}; \\
 B &= \begin{bmatrix} -0.5 \\ 0.0064 \\ 0 \end{bmatrix}; \\
 C &= [2.5 \quad -1 \quad 1.10].
 \end{aligned} \tag{46}$$

To show the identification accuracy of these above identified parameters, we use the Matlab simulation tool to simulate the output response of Bode plot in this state space system, and the phase plot is obtained with amplitude plot simultaneously. To verify the efficiency of the identified mode and make sure that this identified model can be used to replace the true model, we compare the Bode responses

through the true model and its identified model, respectively, in Figure 11, where the red curve denotes the true response and the black curve is the identified response. More specifically, the true response is simulated using the true matrices or parameters, and the black curve is given using our identified matrices or parameters. From Figure 11, we see that the black curve coincides with the red curve; this means that these two Bode response curves coincide with each other, and the model error will converge to zero with increasing time.

As the choice of scaling parameter depends on one criterion function about some estimation in unscented transformation, the maximum likelihood criterion is proposed to obtain one suitable scaling parameter. The maximum likelihood criterion is used to design the optimal scaling parameter, and we use four steps to adjust the optimal scaling parameter. The adjusted result is shown in

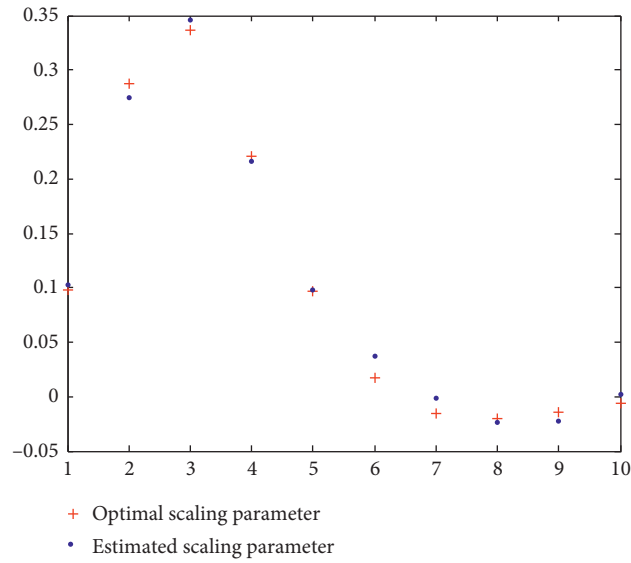
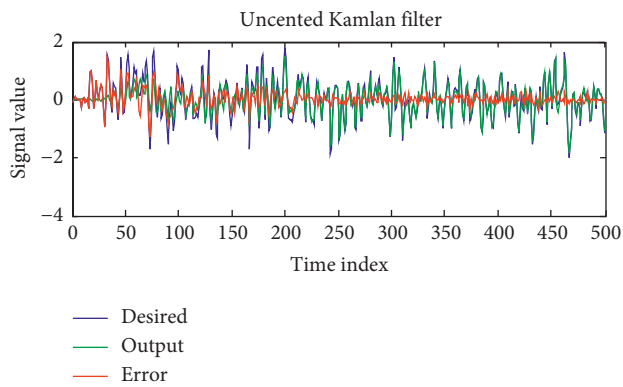
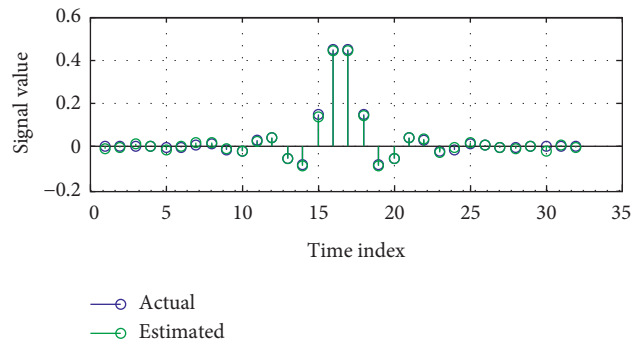


FIGURE 12: Comparison of the optimal scaling parameter and estimated scaling parameter.



(a)



(b)

FIGURE 13: SOC estimation results.

Figure 12, where we compare the optimal scaling parameter and its corresponding estimated scaling parameter at every time instant. From Figure 12, we see that at every time instant, these two kinds of scaling parameters coincide with each other.

In Figure 12, the reason why the two kinds of scaling parameter coincide with each other is that the estimated scaling parameter is obtained by solving one maximum likelihood estimation problem. As this constructed maximum likelihood criterion is one global convex function, its minimum value is unique; i.e., the estimated value is the optimal value.

Now, we start to use our considered improved unscented Kalman filter algorithm, plotted in Figure 4 to estimate SOC. According to the four steps, i.e., initialization, conditional filter, probability update, and combined output. The SOC estimation results are shown in Figure 13, where the black curve is the estimated output and the blue curve is the

desired output for the whole state space system. From Figure 13, it can be seen that the results of SOC estimation using the proposed improved unscented Kalman filter algorithm are close to the desired values. The advantage of our improved unscented Kalman filter algorithm is in introducing one adjustment scaling parameter. This scaling parameter always changes with time instant increase, but not be constant. More specifically, in case of large estimation error, the scaling parameter adjusts adaptively to pull the estimation value near its true value. SOC estimation errors are shown using the red curve, which is also amplified in Figure 14. SOC estimation error is defined as $error = \max|SOC_k - \widehat{SOC}_k|$. From the fact that SOC estimation error curve converges to zero, we see that the SOC estimation can be used to replace the true SOC value; i.e., SOC estimations obtained by our improved unscented Kalman filter algorithm are useful for later control or other fields.

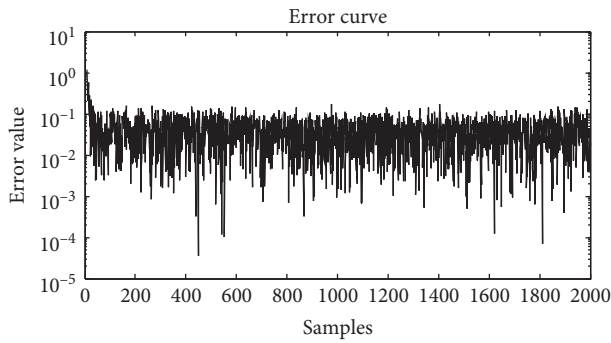


FIGURE 14: SOC estimation error.

7. Conclusion

In this paper, after the equivalent circuit model is used to describe the battery charging and discharging properties, one state space equation is constructed to regard SOC as one state variable. Based on this state space model about SOC, unscented Kalman filter algorithm is proposed to achieve the goal of SOC estimation, and one adjustment strategy for the scaling parameter adaptively is advised for this unscented Kalman filter algorithm. Furthermore, to extend the single SOC estimation to multiple modules, one improved unscented Kalman filter algorithm is studied based on iterative multiple models. Based on our improved algorithms, the sensitivity of model parameter decreases and SOC estimation error converges to zero.

Data Availability

The data used to support the findings of this study are available from the corresponding author upon request.

Conflicts of Interest

The authors declare that they have no conflicts of interest.

References

- [1] M. R. Mohamed, P. K. Leung, and M. H. Sulaiman, "Performance characterization of a vanadium redox flow battery at different operating parameters under a standardized test-bed system," *Applied Energy*, vol. 137, pp. 402–412, 2015.
- [2] M. Guarnieri, P. Mattavelli, G. Petrone, and G. Spagnuolo, "Vanadium redox flow batteries: potentials and challenges of an emerging storage technology," *IEEE Industrial Electronics Magazine*, vol. 10, no. 4, pp. 20–31, 2016.
- [3] W. C. Hong, B. Y. Li, and B. G. Wang, "Theoretical and technological aspects of flow batteries: measurement of state of charge," *Energy Storage Science and Technology*, vol. 56, pp. 744–756, 2015.
- [4] C. Petchsingh, N. Quill, J. T. Joyce et al., "Spectroscopic measurement of state of charge in vanadium flow batteries with an analytical model of VIV-VV absorbance," *Journal of The Electrochemical Society*, vol. 163, no. 1, pp. 5068–5083, 2016.
- [5] X. Li, J. Xiong, A. Tang, Y. Qin, J. Liu, and C. Yan, "Investigation of the use of electrolyte viscosity for online state-of-charge monitoring design in vanadium redox flow battery," *Applied Energy*, vol. 211, pp. 1050–1059, 2018.
- [6] N. Kittima and A. Arpornwichanop, "Measuring the SOC of the electrolyte solution in a vanadium redox flow battery using a four-pole cell device," *Journal of Power Sources*, vol. 298, pp. 150–157, 2015.
- [7] S. Ressel, F. Bill, L. Holtz et al., "State of charge monitoring of vanadium redox flow batteries using half cell potentials and electrolyte density," *Journal of Power Sources*, vol. 378, pp. 776–783, 2018.
- [8] Y. S. Chou, N. Y. Hsu, K. T. Jeng, K.-H. Chen, and S.-C. Yen, "A novel ultrasonic velocity sensing approach to monitoring state of charge of vanadium redox flow battery," *Applied Energy*, vol. 182, pp. 283–289, 2016.
- [9] Q. Zhong, F. Zhong, J. Cheng, H. Li, and S. Zhong, "State of charge estimation of lithium-ion batteries using fractional order sliding mode observer," *ISA Transactions*, vol. 66, pp. 448–459, 2016.
- [10] B. Xiong, J. Zhao, Y. Su, Z. Wei, and M. Skyllas-Kazacos, "State of charge estimation of vanadium redox flow battery based on sliding mode observer and dynamic model including capacity fading factor," *IEEE Transactions on Sustainable Energy*, vol. 8, no. 4, pp. 1658–1667, 2017.
- [11] J. Wang, "Zonotope parameter identification for virtual reference feedback tuning control," *International Journal of Systems Science*, vol. 50, no. 2, pp. 351–364, 2019.
- [12] A. Care, B. Cs, M. C. Campi, and E. Weyer, "Finite-sample system identification: an overview and a new correlation method," *IEEE Control Systems Letters*, vol. 2, no. 1, pp. 61–66, 2018.
- [13] Z. Wei, A. Bhattarai, C. Zou, S. Meng, T. M. Lim, and M. Skyllas-Kazacos, "Real-time monitoring of capacity loss for vanadium redox flow battery," *Journal of Power Sources*, vol. 390, pp. 261–269, 2018.
- [14] C. Lin, H. Mu, and R. Xiong, "A novel multi-model probability battery state of charge estimation approach for electric vehicles using H-infinity algorithm," *Applied Energy*, vol. 344, pp. 195–207, 2017.